

Absolute frequency measurement of the iodine-stabilized Ar<sup>+</sup> laser  
at 514.6 nm using a femtosecond optical frequency comb.

A. GONCHAROV<sup>♦</sup>, A. AMY-KLEIN<sup>\*</sup>, O. LOPEZ, F. DU BURCK and C. CHARDONNET

LPL, Laboratoire de Physique des Lasers, UMR 7538 C.N.R.S., Université Paris 13,  
99, av. J.-B. Clément, 93430 Villetaneuse, France, fax: +33 49 40 32 00.

**Abstract.**

The frequency of <sup>127</sup>I<sub>2</sub> hyperfine component a<sub>3</sub> of the P(13) 43-0 transition at 514.6 nm has been measured with an optical clockwork based on a femtosecond laser frequency comb generator. The measured frequency at an iodine pressure of 0.12 Pa is 67.3(0.75) kHz higher than the value of 582490603.38(15) MHz, adopted by the CIPM in 2003 [T.J. Quinn, *Metrologia* **40**, 103 (2003)] but is in a good agreement with the value measured by *R.J. Jones et al* [*Appl. Phys.* **B74**, 597 (2002)]. In our experiment we used H-maser reference frequency located at BNM-SYRTE Observatoire de Paris and transported to our laboratory by a 43 km optical fibre link.

PACS : 06.20.-f, 06.20.Fn, 06.30.Bp, 06.30.Ft

---

<sup>♦</sup> Permanent address : Institute of Laser Physics, Novosibirsk, Russia, fax: +7 3832 33 20 67

<sup>\*</sup> Corresponding author : fax: +33 1 49 40 32 00, tel : +33 1 49 40 33 79, E-mail: amy@galilee.univ-paris13.fr

## 1 Introduction

The recent advances in optical frequency synthesis and metrology by using femtosecond mode-locked lasers [1-4] as well as progress in microwave frequency standards with cooled atoms [5-7] and cryogenic oscillators [8], opened a promising era in time-frequency standards. The enormous simplification of absolute frequency measurements in the optical range and the possibility of one-step coherent transfer of optical reference stability to the microwave range put optical frequency standards into a new perspective. At the same time the stability of today's primary Cs standard can be transferred relatively easily to the IR, visible and UV spectral ranges and thus intermediates frequency references are not needed any more for precision experiments in the optical range. Nevertheless, developments of relatively simple and cheap transportable secondary laser frequency reference systems are very important for fundamental and practical applications. These systems could have a reproducibility in the range  $10^{-13} - 10^{-14}$  which is better than the usual commercial microwave standards. After frequency calibration with respect to a primary Cs frequency standard they could be used for high precision measurements over all the optical range via a femtosecond frequency comb transfer oscillator.

Secondary laser frequency references based on iodine absorption lines are promising due to their relative simplicity, wide grid of reference lines in the 0.5 – 0.9  $\mu\text{m}$  spectral range, and high frequency reproducibility. The reference lines can be detected with a width of a few hundreds kHz ( $\Delta\nu/\nu \sim 10^{-10}$ ) and even  $\Delta\nu/\nu \sim 10^{-11}$  near the dissociation limit ( $\lambda \approx 500 \text{ nm}$ ), which gives the possibility to obtain frequency reproducibility at the level of  $10^{-13}$ . As a matter of fact the CIPM is recommending 7 laser sources for the realization of the metre using iodine reference lines for frequency stabilization [9]. Until recently the choice of the iodine line for frequency stabilization was motivated by the existence of acceptable laser sources and CIPM recommends mostly He-Ne lasers. However, due to fast progress in the fields of diode lasers, diode pumped solid state lasers and non-linear optics, systematic search of the best iodine reference line is in progress now [10]. Today's most promising standard based on the iodine reference is the  $\text{Nd}^{+3}$ :YAG/SHG diode pumped laser at 532 nm [11-14], even though the reference line is still broad in this case (approx. 250 kHz). The most interesting spectral range is 500 – 520 nm near dissociation limit of  $\text{I}_2$ . Owing to the increase of the iodine B state lifetime [15-16] reference lines may have widths of a few kHz [10]. For example, the natural width of the  $a_2$  hfs component of P(13) 43-0 transition at 514.6 nm is 48 kHz [17]. The width

of the saturated absorption resonance at 62-0 R(26) at 501.7 nm was measured to be less than 28 kHz [18].

A large number of iodine spectroscopic data gives the possibility to identify a particular iodine line and a hyperfine structure (hfs) component and to calculate the frequency of hfs components with an accuracy better than 0.2 MHz in the range 776 – 815 nm, 3 MHz in the range 526 – 667 nm and 30 MHz in the ranges 515 – 526 nm and 667-676 nm [19]. To increase this accuracy, especially in the most interesting and less explored range, measurements of absolute frequency of iodine lines are required. Before the era of femtosecond frequency comb metrology the frequencies of iodine lines at 633 nm [20-21], 532 nm [11], 576 nm [22] and 815 nm [23] were measured with a conventional frequency divide chain or using combinations of earlier measured optical frequency standards. With fs comb generators (FCG) the frequencies of iodine stabilized lasers at 532 nm [24-26], 633 nm [27-28] and recently at 515 nm [29] were measured.

In this paper we present an absolute frequency measurement of the  $\text{Ar}^+$  - laser frequency stabilized to iodine hyperfine component  $a_3$  of P(13) 43-0 line at 514.6 nm in a low pressure iodine cell. We used the techniques of self-reference [30-31] and of transfer oscillator [32-33] to measure the  $\text{Ar}^+/\text{I}_2$  frequency with only one counting channel system, without stabilization of carrier-envelope frequency offset,  $f_0$ , and without another absolute optical frequency reference. We also demonstrate an “optical clock” when the repetition rate  $f_{\text{rep}}$  of the fs laser was stabilized to the frequency of  $\text{Ar}^+/\text{I}_2$  –frequency standard. The measurements were carried out using the BNM-SYRTE<sup>1</sup> primary frequency standard, the metrological properties of which being transmitted to LPL with a long-distance optical link [34].

## 2 $\text{Ar}^+/\text{I}_2$ frequency standard.

The  $\text{Ar}^+/\text{I}_2$  stabilization set-up was developed many years ago [35], and recently was modified for ultrahigh resolution Raman spectroscopy of iodine [36]. A specificity of the set-up is the 4 m long low pressure iodine cell which gives the possibility to observe high contrast saturation resonances with iodine pressure in the range 0.01 – 0.1 Pa. The cell is not sealed and may be pumped during experiment to minimize buffer gases and impurities. Our experiments on Raman spectroscopy of iodine in this cell demonstrate resonance widths of

---

<sup>1</sup> BNM-SYRTE, UMR 8630 CNRS, Observatoire de Paris, 61 avenue de l'Observatoire 75014 Paris, France

2.6 kHz, that indicate an upper limit of residual buffer gases and impurity pressure less than 0.04 Pa [36]. The experimental set up is shown in Fig 1.

The linewidth of the single mode Ar<sup>+</sup> - laser (Spectra Physics - 2020-5) operating at 514.6 nm is reduced when its frequency is locked onto a mode of a highly stable Fabry-Perot interferometer detected in reflection with the Pound-Drever-Hall method. The laser line width was estimated to 20 kHz, mainly limited by the stability of the Fabry-Perot interferometer itself. The Ar<sup>+</sup> laser frequency is then stabilized onto the iodine a<sub>3</sub> hfs component of 43-0 P(13) transition at 514.6 nm, detected in saturated absorption spectroscopy. The probe beam frequency is modulated at 2.5 MHz with an acousto-optic modulator (AOM). A system for the narrow-band control of the beam intensity at the modulation frequency is used for the rejection of the residual amplitude modulation generated by the AOM [37]. Phase sensitive detection of the probe beam at 2.5 MHz gives an error signal with a dispersion shape. An additional amplitude modulation of the saturation beam at 5 kHz and a second phase sensitive detection were used to eliminate the residual offset of the error signal due to the Doppler background. Fig.2 displays the error signal obtained with an iodine pressure of 0.12 Pa, probe and saturation beam powers equal to 0.8 and 2 mW respectively, and beam diameters of 6 mm.

The correction signal for frequency stabilization is applied to the piezoceramic transducer (pzt) which controls the length of the Fabry-Perot interferometer. Bandwidth of the correction loop is approximately 100 Hz. For absolute frequency measurement, a small amount of Ar<sup>+</sup> - laser power (approx. 10 mW) was directed along a 20 m polarization maintaining single mode fibre (PMSMF) to the experimental room where the femtosecond comb generator set-up was located.

### **3 Frequency measurement procedure and femtosecond comb generator (FCG) set up.**

#### ***3.1 Principle of measurement***

The scheme of our FCG is similar to many existing setups for absolute frequency measurements with femtosecond lasers. The principle of absolute frequency measurement is based on the property that the frequency of any particular mode of the femtosecond comb is given at every moment with an extremely high relative accuracy  $\sim 10^{-18}$  [33] by the equation:

$$f_p(t) = f_0(t) + p f_{\text{rep}}(t), \quad (1)$$

where  $f_0$  is the carrier-envelope offset frequency [38],  $f_{\text{rep}}$  is the repetition rate of fs laser. To measure a frequency  $f_x$ , one has to compare it with a primary frequency standard. If the fs comb delivers sufficient power near the frequency  $f_x$ , the beat signal  $\delta(t) = |f_x - f_p(t)|$  as well as  $f_{\text{rep}}(t)$  and  $f_0(t)$  could be controlled with respect to the primary frequency standard to measure  $f_x$ :

$$f_x = f_0(t) + p f_{\text{rep}}(t) \pm \delta(t) \quad (2)$$

The problem of the uncertainty of the integer  $p$  has to be solved by  $f_x$  pre-measurement with an uncertainty  $\Delta f_x / f_x$  of the order of  $f_{\text{rep}} / f_x \approx 10^{-6} - 10^{-7}$ , which is easily done with commercial lambdameters. The  $(\pm)$  indetermination in the equation (2) may be removed by varying  $f_{\text{rep}}$ . To control  $f_0$ , the self-reference technique of FCG may be used [30]. It used nonlinear optical processes for phase-coherent transfer of one or several parts of the comb to the same frequency domain or to a frequency domain where initial comb has enough power density. Information about  $f_0$  is then given by a beat note signal. The simplest case may be realized when the initial comb spans more than one octave [31]. Thus the second harmonic (SH) of the low frequency wing of the comb can overlap the high frequency wing, and their beat notes gives directly  $f_0$ :

$$2(f_0(t) + p f_{\text{rep}}(t)) - (f_0(t) + 2p f_{\text{rep}}(t)) = f_0(t).$$

If signals  $f_0(t)$ ,  $f_{\text{rep}}(t)$ ,  $\delta(t)$  are detected with a high S/N ratio (more than 30-40 dB in a few hundred kHz bandwidth), it is possible to measure the frequency ratio  $f_x / f_{\text{ref}}$  of two frequencies  $f_x$  (unknown) and  $f_{\text{ref}}$  (reference frequency) with an accuracy much higher than the relative accuracy of the primary frequency standard. In this case, real time signal processing as mixing and direct-digital synthesis, are needed without measurements or a phase-lock controlling of  $f_0$  and  $f_{\text{rep}}$ . Control of  $f_{\text{ref}}$  with the accuracy of the primary frequency standard will give the optical frequency  $f_x$  with the accuracy of the primary standard. In this case the concept of optical transfer oscillator based on FCG is fully realized [32]. It is a very important point that this allows comparison of frequencies, via a frequency ratio, of different frequency standards with an extremely high precision. As a result, this can improve the accuracy of fundamental constants variation experiments [39].

Following the concept of transfer oscillator, the signals  $f_0(t)$  and  $\delta(t)$  are mixed by a double balance mixer (DBM) to obtain the signal :  $\Delta(t) = f_0(t) \pm \delta(t)$ . According to equation (2), with a proper choice of DBM output :

$$\Delta(t) = f_x - p f_{\text{rep}}(t), \quad (3)$$

which will not depend anymore on  $f_0(t)$ , and there is no need to measure or stabilize  $f_0$ .

The most critical value is  $f_{\text{rep}}$  as it is multiplied by a factor  $N \approx 10^5 - 10^6$  in equation (2), when the visible frequency is measured with a fs laser of  $f_{\text{rep}} \approx 10^8 - 10^9$  Hz. If  $f_{\text{rep}}$  is controlled by phase locking to a local oscillator (LO) then, after multiplication of LO phase noise spectral density by factor  $N^2$ , this noise becomes a frequency noise in the optical domain [40]. This phenomenon restricts the servo loop bandwidth, and, as a result, the accuracy of the measurement, which would require a longer measurement time. An extremely high quality of LO is needed for this scheme.

To measure the absolute frequency  $f_x$ , one needs either to lock  $f_{\text{rep}}$  to a LO controlled by a primary frequency standard and count  $\Delta(t)$ , or to use the signal  $\Delta(t)$  for locking  $f_{\text{rep}}$  to the optical frequency standard and to count  $f_{\text{rep}}$ . In the first case phase noise of LO is a serious problem as discussed above. In the second case the fs comb generator works as a coherent optical divider which transfers the metrological properties of the optical standard to the radio frequency range : an “optical clock” is realized. This is a way to develop a radio frequency oscillator with low phase noise and ultrahigh short term stability.

In our set up we used and compared these methods to measure the frequency of  $\text{Ar}^+/\text{I}_2$  stabilized laser.

### 3.2 *Experimental set-up*

Fig. 3 shows the scheme of our set-up. Our femtosecond optical comb was produced with a 1 GHz repetition rate Ti:Sa laser (GigaJet) [41] and a photonic crystal fibre (PCF) [42]. When pumped by 5W of frequency-doubled Nd:YVO<sub>4</sub> laser (Verdi V), the fs laser generates an average power of about 650 mW. Approximately 30% - 40% of the laser output power was injected into a 25-30 cm long PCF with a core diameter 2  $\mu\text{m}$  with  $f = 2.75$  mm aspherical lens L1. A  $\lambda/2$  plate was used to control the spectrum at the PCF output, which is sensitive to the input laser polarization. PCF with core diameters 1.8, 2 and 2.25  $\mu\text{m}$  were tested. It was observed that initial pulse broadening to the visible part of the spectrum is more sensitive to fibre core diameter and less sensitive to fibre length. By contrast, spectral broadening to the infrared part is sensitive to fibre length. Output spectra suitable for our measurements were obtained with fibres of diameter 2 and 2.25  $\mu\text{m}$  and length 20-30 cm. Fig. 4 shows PCF output spectrum for a core diameter of 2  $\mu\text{m}$  and a length of 25 cm.

The output beam from the PCF was collimated with a second aspherical lens L2. Actually only the visible part of PCF output was collimated while, due to chromatic aberration, the infrared part was slightly divergent. The infrared part of the spectrum was separated from the

visible part with a dichroic mirror and, after frequency doubling in a 5 mm long LBO crystal, was combined with the visible part of the PCF output beam to obtain the beat note at frequency  $f_0$ . Two lenses L3 and L4 with  $f=10$  cm were used to focus the IR radiation into the non-linear crystal and to collimate the green SH radiation after crystal. The LBO crystal was cut for critical phase matching at  $\lambda=1$   $\mu\text{m}$ . By tuning the crystal around its Z-axis it was possible to adjust the phase matching conditions in the range of 0.95 - 1.05  $\mu\text{m}$ . In our case the IR radiation centred at 1.03  $\mu\text{m}$  is doubled to visible range with a bandwidth of  $\sim 5$  nm. A variable optical delay (VD) was used to match the optical path lengths of both arms of the interferometer with an accuracy of 10  $\mu\text{m}$ , and thus to overlap temporally both pulses from both arms. A 1200 l/mm grating was used for spectral filtering of radiation going to the fast PIN photodiode (PD) to reduce the background noise and the large signal at 1 GHz. The  $f_0$  signal varies from 200 to 400 MHz depending on the Ti:Sa cavity adjustment. It was detected with a S/N of  $\sim 40$  dB in 100 kHz bandwidth. Approximately 5 mW of  $\text{Ar}^+$ -laser radiation after PMSMF was matched with the green part of the comb to get the beat note (signal at frequency  $\delta$ ). A spectral filtering with grating was also used to reduce the background noise and the large signal at 1 GHz. Usually S/N was 35 dB in 100 kHz bandwidth. Then the signals “ $\delta$ ” and “ $f_0$ ” were amplified up to level of 0 dBm, and mixed in a double balance mixer (DBM). The output signal at  $|\delta - f_0|$  was filtered with a band pass filter (BPF) at 21.4 MHz. The  $|\delta - f_0|$  frequency was tuned to the BPF centre by adjusting the repetition rate  $f_{\text{rep}}$  by changing the Ti:Sa cavity length with pzt. After amplification this signal with S/N  $\sim 35$  dB was directed to either a high resolution counter HP/Agilent 53132A or the GigaJet pzt to phase-lock the repetition rate to  $\text{Ar}^+/\text{I}_2$  –frequency standard (see fig.3).

The repetition rate  $f_{\text{rep}}$  of the Ti:Sa laser was detected with a fast PIN PD. Its output was mixed with the signal from a RF synthesizer ROHDE&SCHWARZ SML 01 (R&S) operating at  $\sim 1$  GHz to get a signal in the RF range. This signal  $|f_{\text{synth}} - f_{\text{rep}}|$  was used either for phase locking the repetition rate to the R&S synthesizer (in this case  $f_{\text{rep}} = f_{\text{synth}}$ ) or for frequency measurement with the counter. All the RF synthesizers and the counter were locked to a 10 MHz local oscillator (LO) produced with the second harmonic of a high quality low phase noise quartz oscillator. This LO was locked to the BNM- SYRTE primary frequency standard [34]. RF signal with the metrological characteristics of the BNM- SYRTE primary frequency standard was transmitted to our laboratory via a 43 km optical fibre. The complete optical link includes a distributed feedback (DFB) semiconductor laser ( $\lambda=1.55$   $\mu\text{m}$ ) located in BNM- SYRTE, a 43 km optical fibre and a PIN photodiode located in our laboratory. The

DFB laser current is modulated at 100 MHz directly controlled by the BNM- SYRTE H-Maser. The amplitude modulation is detected by the PIN PD at the output of the link and a quartz oscillator at 5 MHz was locked to this signal.

### 3.3 *Measurement procedure*

Two methods were used to measure the  $\text{Ar}^+/\text{I}_2$  frequency. First we locked the repetition rate of the fs laser to the R&S synthesizer (switches in position 1 at fig. 3 ) and the signal  $|\delta - f_0| \approx 21.5$  MHz was counted. Fig.5 shows the power density spectrum of this signal detected with a spectrum analyser (SA). The solid line corresponds to the case when the repetition rate is locked to the R&S synthesizer with a servo loop bandwidth of  $\sim 1$  kHz. This bandwidth was optimised to obtain the narrowest spectrum for the signal. When increasing the bandwidth, the spectrum becomes larger due to the transformation of the RF synthesizer phase noise to jitter of the fs laser comb. With a lower bandwidth, acoustic perturbations in the laboratory becomes the dominant contribution in spectral broadening.

The signal  $|\delta - f_0|$  was counted with a counter gate of 1 s. The counter was controlled by a computer which calculated the mean frequency and the Allan deviation from a series of 1 s gate measurements. In these measurements we did not use any tracking oscillator or any system of control of cycle-slips in the PLL. We only removed at the end of the measurement procedure the few points whose frequencies differ more than  $\sim 10 \sigma$  from the mean frequency, where  $\sigma$  is the standard deviation for a 1 s measurement.

In the second method (switches in position 2 at fig. 3 ), the frequency of the signal  $|\delta - f_0|$  was divided by 64 in order to phase-lock the  $\sim 581840$ -th harmonic of the repetition rate to the  $\text{Ar}^+/\text{I}_2$  stabilized laser frequency. The 64-time frequency divider was used to increase the dynamical range of the PLL system. The servo-loop bandwidth in this case was  $\sim 10$  kHz and was limited by the dynamical properties of the Ti:Sa laser's pzt. Dashed line in Fig.5 shows power density spectrum of  $|\delta - f_0|$  signal detected with a spectrum analyser when the servo-loop is closed. The spectral width is much narrower than in the first case. The difference  $|f_{\text{synth}} - f_{\text{rep}}|$  was counted, with 1s gate, at a frequency of a few kHz. Since the servo loop bandwidth is 10 times larger, this second method of measurement is less sensitive to the acoustic and vibration perturbations in the laboratory. Fig. 6 shows the time record of  $|f_{\text{synth}} - f_{\text{rep}}|$  multiplied by the factor 581840, to carry out frequency-scale to optical frequency domain ( $\text{Ar}^+/\text{I}_2$  laser frequency).



The phase noise of the synthesizer is still important for this measurement. To check its effect on the measurement stability, we perform the same experiment with two R&S synthesizers. The signals from both R&S synthesizers at  $\sim 1$  GHz with a frequency difference of a few kHz were mixed in a DBM and their frequency difference was counted. Fig 7 shows the corresponding Allan deviation (up and down triangles), together with the Allan deviation of the  $\text{Ar}^+/\text{I}_2$  frequency measurement (circles).

From this experiment it is clear that in the present measurements the Allan deviation is limited by the stability of the  $\text{Ar}^+/\text{I}_2$  laser. The phase noise of the R&S synthesizer limits the stability at the level of  $3 \cdot 10^{-13}$  for 1-s averaging time, that is more than 3 times larger than the stability of BNM-SYRTE frequency standard. Another important point is that it is better to make the counting gate 10 – 100 s rather than 1s for a signal with phase noise [43]. This is due to the dead time between each 1 s measurement [44]. When the gate time equals averaging time, we observe the expected  $\tau^{-1}$  dependence of the Allan deviation. With gate time more than  $\sim 30$  s phase noise of R&S synthesizer will not limit the measurement accuracy.

#### 4 Experimental results

For the present measurements we used time series of 1 s gate samples because it was convenient to display measurement frequency in real time in order to remove “bad” points caused by acoustic and vibration perturbation or to stop measurement when PLL got unlocked. It was especially important in the case of the first measurement method. The usual measurement procedure comprised averaging of few hundred 1s gate points with standard Allan deviation of  $\sigma_y \approx 400$  Hz when converted to the optical frequency range. Up to 10 measurements were obtained in one day and the mean frequency values for several days are shown in fig.8.

During a period of 1 week we switched between the two methods of measurements and did not found any frequency difference higher than the uncertainty. At the present stage of the  $\text{Ar}^+/\text{I}_2$  frequency stability the two methods of measurement give the same result, except that the second method demonstrates higher stability to acoustic and vibration perturbations in the laboratory. Note that, in fact, with the second method, we transfer the stability of the optical standard to the RF frequency range and that is a realisation of a “molecular optical clock”.

The mean frequency over all the measurement was found to be  $\langle \nu_{\text{meas}} \rangle = 582\,490\,603\,447.3$  (0.24) kHz. The uncertainty is the pure statistical  $1\sigma$ .

It is clear from Fig. 8 that the frequency measured on each day depends on the daily experimental parameters. We carried out preliminary studies of  $\text{Ar}^+/\text{I}_2$  stabilized laser frequency shift on the parameters of frequency stabilization setup - power of the probe and saturated beam, amplitude of modulation. Changing these parameters by factor 2 we did not find any frequency shift larger than 0.5 kHz. Note that this technique of absolute frequency measurement gives an unique possibility to study frequency shifts if only one laser system is available.

The comparison with the value adopted by CIPM [9] gives  $\langle \nu_{\text{meas}} \rangle - \nu_{\text{CIPM}} = \Delta = +67.3$  (0.7) kHz. We give a conservative uncertainty of  $3\sigma$  for the reproducibility of our measurement. Since  $\nu_{\text{CIPM}}$  is given for iodine pressure  $P_{\text{I}_2} = 2.38$  Pa ( $t = -5^\circ\text{C}$ ), our value measured at 0.12 Pa has to be extrapolated to “standard” conditions. With the long cell of our set-up it was not possible to measure pressure shift directly since the absorption is too high at iodine pressure of  $\sim 2$  Pa. In [29] a pressure shift of  $\delta\nu/\delta P_{\text{I}_2} = -2.5 \pm 0.5$  kHz/Pa was measured with short  $\text{I}_2$  cell. Using this data, extrapolation of our measurement to pressure of 2.38 Pa will give  $\Delta = 61.7 \pm 1.3$  kHz. Earlier studies of pressure shift of  $\text{I}_2$  saturation resonance at  $a_2$  hfs component were carried out in [45,46]. At low pressure (less than 2.7 Pa), the unresolved recoil doublet is not symmetric anymore. The amplitude of the low-frequency component decreases, because this resonance involves a population of the excited level, the lifetime of which is shorter than the coherent interaction time given by the laser linewidth, the transit width or the pressure width. The frequency shift shows non-linear dependence on pressure well described by:

$$\delta\nu(P_{\text{I}_2}) = \delta_{\text{recoil}}[\Gamma_e(P_{\text{I}_2}) - \Gamma_g(P_{\text{I}_2})] / [\Gamma_e(P_{\text{I}_2}) + \Gamma_g(P_{\text{I}_2})] - (1.5 \text{ kHz/Pa}) P_{\text{I}_2},$$

where  $\delta_{\text{recoil}} = h\nu^2/2Mc^2 \approx 3.0$  kHz is recoil shift,  $\Gamma_e$  and  $\Gamma_g$  are the widths of the excited and ground states respectively, with  $\Gamma_e(P_{\text{I}_2}) = \Gamma_{\text{natural}} + (130 \text{ kHz/Pa}) P_{\text{I}_2}$  and  $\Gamma_g(P_{\text{I}_2}) = \Gamma_{\text{transit}} + (95 \text{ kHz/Pa}) P_{\text{I}_2}$ . For our experimental conditions  $\Gamma_{\text{transit}} \approx 10$  kHz and  $\Gamma_{\text{natural}} \approx 130$  kHz. Fig. 9 shows the calculated frequency shift as a function of iodine pressure.

Taking into account this pressure shift, we have to correct our measurement value  $\Delta$  by  $-4.7$  kHz and the extrapolation gives the value  $\Delta = 62.6$  (0.7) kHz. This has to be

compared with the former measurement in [29] which gives  $\Delta = 61.8 (1.5) \text{ kHz}^2$ . As a result, the present measurement value of the frequency of hfs component  $a_3$  well coincide with the value given in [29] with the uncertainty of less than 1.5 kHz.

## 5 Conclusion.

The absolute frequency measurement of the  $^{127}\text{I}_2$  hyperfine component  $a_3$  of the P(13) 43-0 transition at 514.6 nm with a fs comb generator was carried out. This measurement coincides within less than 1 kHz with the measurement developed in [29]. Current accuracy limitation is the frequency stability and reproducibility of our  $\text{Ar}^+/\text{I}_2$  frequency standard. The technique of optical transfer oscillator was used to measure absolute frequency without stabilization or measurement of the carrier-envelope offset frequency  $f_0$ . Two methods of measurement were developed for which the repetition rate  $f_{\text{rep}}$  of the fs laser either was locked to RF local oscillator or was stabilized to the frequency of  $\text{Ar}^+/\text{I}_2$  –frequency standard. At the present level of uncertainty two methods gave the same result except that the second method demonstrates higher stability to acoustic and vibration perturbations in the laboratory.

## Acknowledgement

The authors would like to thank Jonathan Knight from Bath University for providing several pieces of photonic crystal fibres.

The authors would like to thank the Ministère de la Recherche and the CNRS for specific funds. A.G. would like to thank University Paris 13 for its hospitality and financial support.

---

<sup>2</sup> Note that in [29] authors gave the value  $\Delta = 71.8 \pm 1.5 \text{ kHz}$  with respect to previous definition of  $a_3$  frequency  $\nu_{a_3} = 582\,490\,603\,370 \pm 150 \text{ kHz}$  [T.J. Quinn: Metrologia **36**, 211 (1999)]

With the new definition of [9] this value is 10 kHz higher

## References

1. R. Holzwarth, M. Zimmermann, T. Udem, and T.W. Hänsch: IEEE J. Quant. Electron. **37**, 1493 (2001), and references therein;
2. L. Hollberg, C.W. Oates, E.A. Curtis, E.N. Ivanov, S.A. Diddams, T. Udem, H.G. Robinson, J.C. Bergquist, R.J. Rafac, W.M. Itano, R.E. Drullinger, and D.J. Wineland: IEEE J. Quant. Electron. **37**, 1502 (2001), and references therein;
3. J.L. Hall, J. Ye, S.A. Diddams, L.-S. Ma, S.T. Cundiff, and D.J. Jones: IEEE J. Quant. Electron. **37**, 1482 (2001), and references therein;
4. S.T. Cundiff and J. Ye, Rev. of Mod. Phys. **75**, 325 (2003), and reference therein;
5. Y. Sortais, S. Bize, M. Abgrall, S. Zhang, C. Nicolas, C. Mandache, P. Lemonde, P. Laurent, G. Santarelli, N. Dimarcq, P. Petit, A. Clairon, A. Mann, A. Luiten, S. Chang, and C. Salomon : Phys. Scr. **T95**, 50 (2001);
6. D. M. Meekhof, S. R. Jeers, M. Stepanovich, T. E. Parker: IEEE Trans. Instrum. Meas. **50**, 507 (2001);
7. S. Weyers, U. Hübner, R. Schröder, C. Tamm and A. Bauch: Metrologia **38**, 343 (2001);
8. A. G. Mann, C. Sheng, and A.N. Luiten: IEEE Trans. Instrum. Meas., **50**, 519 (2001);
9. T.J. Quinn: Metrologia **40**, 103 (2003);
10. W.-Y. Cheng, L. Chen, T.H. Yoon, J.L. Hall, J. Ye: Opt. Lett. **27**, 571 (2002);
11. J.L. Hall, L.-S. Ma, M. Taubman, B. Tiemann, F.-L. Hong, O. Pfister, J. Ye: IEEE Trans. Instrum. Meas. **48**, 583 (1999)
12. J. Ye, L. Robertsson, S. Picard, L.-S. Ma, J.L. Hall: IEEE Trans. Instrum. Meas. **48**, 544(1999);
13. M.V. Okhapkin, M.N. Skvortsov, A.M. Belkin, N.L. Kvashnin, S.N. Bagayev: Opt. Comm. **203**, 359 (2002);
14. P. Cordiale, G. Galzerano and H. Schnatz: Metrologia **37**, 177 (2000);
15. J.C. Keller, M. Broyer, J.C. Lehmann: C.R.A.S.(Paris) **B277**, 369 (1973);
16. J. Vigué, M. Broyer, and J.C. Lehmann: J. Phys. **42**, 937 (1981);
17. C.J. Bordé, G. Camy, and B. Decomps: Phys. Rev. A **20**, 254 (1977);
18. F. du Burck, J.-P. Wallerand, A.N. Goncharov, M. Himbert and Ch. J. Bordé: *Recent progress in ultra-high resolution spectroscopy of molecular iodine*, in *Laser Spectroscopy XII*, ed. by M. Inguscio et al (World Scientific, Londres 1995) p. 220;
19. see [www.toptica.com](http://www.toptica.com), Iodine Spectrum Calculating software - IodineSpec 4;

20. D. A. Jennings, C. R. Pollock, F. R. Petersen, R. E. Drullinger, K. M. Evenson, J. S. Wells, J. L. Hall, H. P. Layer: *Opt. Lett.* **8**, 136 (1983);
21. O. Acef, J. J. Zondy, M. Abed, D. G. Rovera, A. H. Gérard and A. Clairon, Ph. Laurent, Y. Millerieux and P. Juncar: *Opt. Commun.* **97**, 29 (1993);
22. C. R. Pollock, D. A. Jennings, F. R. Petersen, J. S. Wells, R. E. Drullinger, E. C. Beaty, K. M. Evenson: *Opt. Lett.* **8**, 133 (1983);
23. B. Bodermann, M. Klug, H. Knöckel, E. Tiemann, T. Trebst, H. R. Telle: *Appl. Phys. B* **67**, 95 (1998);
24. R. Holzwarth, A. Yu. Nevsky, M. Zimmermann, T. Udem, T. W. Hansch, J. Von Zanthier, H. Walther, J. C. Knight, W. J. Wadsworth, P. St. J. Russell, M. N. Skvortsov, S. N. Bagayev: *Appl. Phys. B* **73**, 269 (2001)
25. S. A. Diddams, D. J. Jones, J. Ye, S. T. Cundiff, and J. L. Hall: *Phys. Rev. Lett.* **84**, 5102 (2000);
26. G. D. Rovera, F. Ducos, J. J. Zondy, O. Acef, J. P. Wallerand: *Meas. Sci. Technol.* **13**, 918 (2002);
27. L.-S. Ma, L. Robertsson, S. Picard, J.-M. Chartier, H. Karisson, E. Prieto, R. S. Windeler: *IEEE Trans. Instrum. Meas.* **52**, 232 (2003);
28. T. H. Yoon, J. Ye, J. L. Hall, J.-M. Chartier: *Appl. Phys. B* **72**, 221 (2001);
29. R. J. Jones, W.-Y. Cheng, K. W. Holman, L. Chen, J. L. Hall, J. Ye: *Appl. Phys.* **B74**, 597 (2002);
30. H. R. Telle, G. Steinmeyer, A. E. Duplop, J. Stenger, D. H. Sutter, U. Keller: *Appl. Phys. B* **69**, 327 (1999);
31. D. J. Jones, S. A. Diddams, J. K. Ranka, A. Stentz, R. S. Windeler, J. L. Hall, and S. T. Cundiff: *Science* **288**, 635 (2000);
32. H. R. Telle, B. Lipphardt, J. Stenger: *Appl. Phys. B* **74**, 1 (2002);
33. J. Stenger, H. Schnatz, C. Tamm, and H. R. Telle: *Phys. Rev. Lett.* **88**, 073601-3 (2002);
34. A. Amy-Klein, A. Goncharov, C. Daussy, C. Grain, O. Lopez, G. Santarelli, C. Chardonnet: *Appl. Phys. B*, (in press);
35. G. Camy, D. Pinaud, N. Courtier and H. C. Chuan: *Revue Phys. Appl.* **17**, 357 (1982);
36. J.-P. Wallerand, F. du Burck, B. Mercier, A. N. Goncharov, M. Himbert and Ch. J. Bordé: *Eur. Phys. J. D* **6**, 63 (1999);
37. F. du Burck, O. Lopez, and A. El Basri : *IEEE Trans. Instrum. Meas.* **52**, 288 (2003);
38. S. T. Cundiff, J. Ye, and J. L. Hall: *Rev. Sci. Instrum.* **72**, 3749 (2001);

39. S.G. Karshenboim: *Can. J. Phys.* **78**, 639 (2000);
40. G.D. Rovera and O. Acef: *Optical frequency measurements relying on a mid-infrared frequency standard*, in *Frequency measurement and Control*, ed. A.N. Luiten (Springer-Verlag, Berlin Heidelberg 2001) p. 249;
41. A. Bartels, T. Dekorsy and H. Kurz: *Opt. Lett.* **24**, 996 (1999),  
Ultracompact femtosecond Ti:Sapphire laser GigaJet was delivered by GigaOptics GmbH;
42. T.A. Birks, J.C. Knight and P.St.J. Russell: *Opt. Lett.* **22**, 961 (1997),  
Cobweb Photonic Crystal Fibres were freely provided by Departure of Physics University of Bath;
43. S. A. Diddams, L. Hollberg, L.-S. Ma, L. Robertsson: *Opt. Lett.* **27**, 58 (2002);
44. P. Lesage: *IEEE Trans. Instrum. Meas.* **32**, 204 (1983);
45. A.N. Goncharov, M.N. Skvortsov, and V.P. Chebotaev: *Appl. Phys. B* **51**, 108 (1990);
46. V.P. Chebotayev, V.G. Goldort, A.N. Goncharov, A.E. Ohm, and M.N. Skvortsov: *Metrologia* **27**, 61 (1990).

## Figure caption.

Fig. 1  $\text{Ar}^+/\text{I}_2$  setup. PD : photodiode, AOM : acoustooptic modulator

Fig 2. Error signal for frequency stabilization of  $\text{Ar}^+$  - laser at 514.6 nm. Time constant of lock-in-amplifier was  $\tau = 10$  ms.

Fig. 3 Femtosecond comb generator set up for frequency measurement of  $\text{Ar}^+/\text{I}_2$  -laser. PC : personal computer, SA : spectrum analyser.

Fig. 4 PCF output “continuum” spectrum : dashed line is the initial spectrum of the femtosecond laser, not scaled. An insert shows the spectrum in vicinity of 514.6 nm. The spectrum was recorded with a compact spectrometer (Ocean Optics HR 2000).

Fig. 5 Power density spectrum of  $|\delta - f_0|$  signal. Solid line – repetition rate was locked to R&S synthesizer, dashed line –  $\sim 581840$ -th harmonic of repetition rate was locked to the frequency of  $\text{Ar}^+/\text{I}_2$  stabilized laser. The spectrum analyser parameters were: resolution bandwidth (rbw) – 30 kHz, video bandwidth (vbw) – 100 kHz.

Fig.6 Time record of 1s gate counting of signal at frequency  $(f_{\text{rep}} - f_{\text{synth}})$  multiplied by factor 581840. The corresponding relative Allan deviation is shown on fig.7.

Fig. 7. Relative Allan deviation of  $\text{Ar}^+/\text{I}_2$  frequency measurements, circles with error bars, calculated from 1 s measurements (Fig. 6). Solid line is the Allan deviation of BNM-SYRTE frequency standard used as reference for our measurements, down triangles – Allan deviation function of R&S synthesizers at  $\sim 1$ GHz calculated from series of 1 s gate counting, up triangles - Allan deviation function of R&S synthesizers at  $\sim 1$ GHz with gate time of counter equal to averaging time.

Fig 8. Frequency difference of the  $\text{Ar}^+/\text{I}_2$  measured value ( $\nu_{\text{meas}}$ ) and the value ( $\nu_{\text{CIPM}}$ ) adopted by the CIPM in 2003 [9] : 582490603.38(15) MHz.  $\text{I}_2$  pressure in the cell was 0.12 Pa.

Fig.9 Calculated frequency shift of the the  $a_3$  hfs component with  $\text{I}_2$  pressure, from [46] with present experimental conditions.

Figure 1

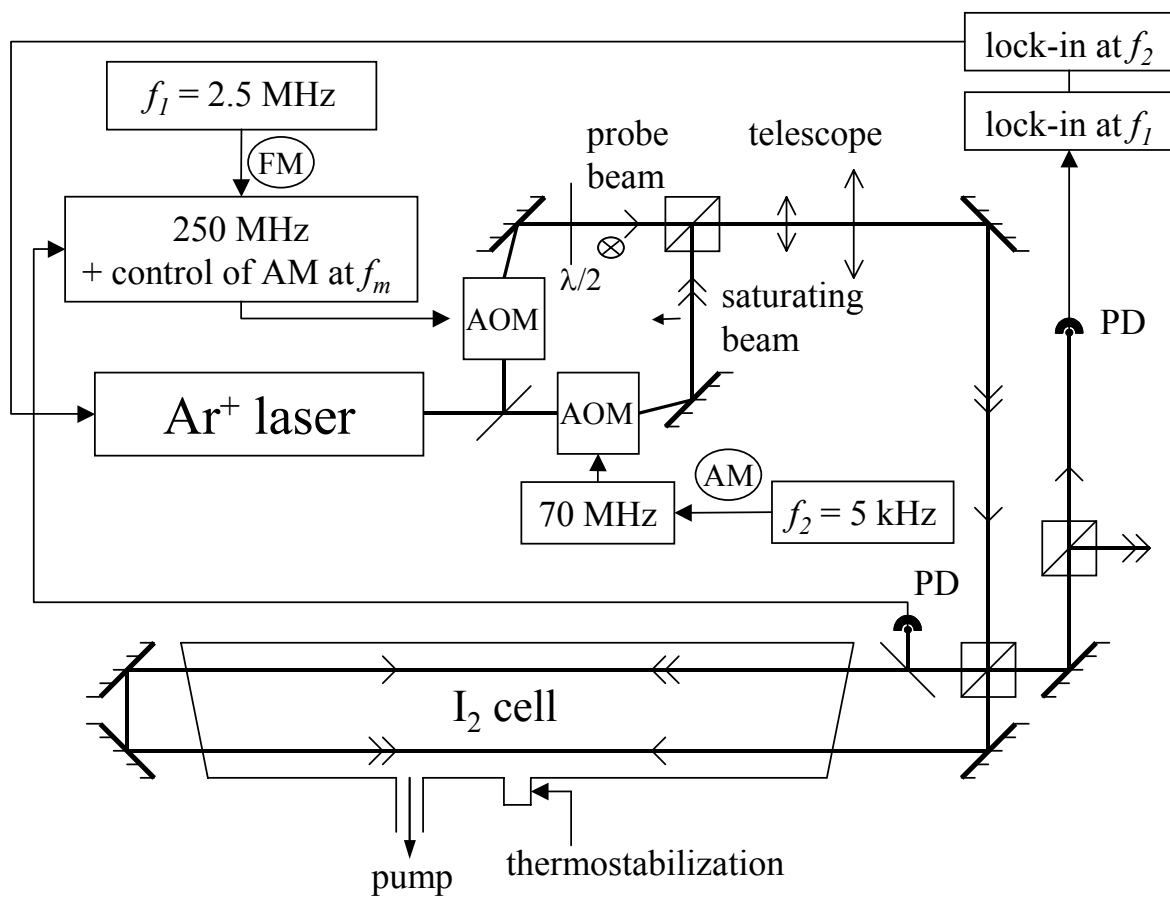




Figure 2

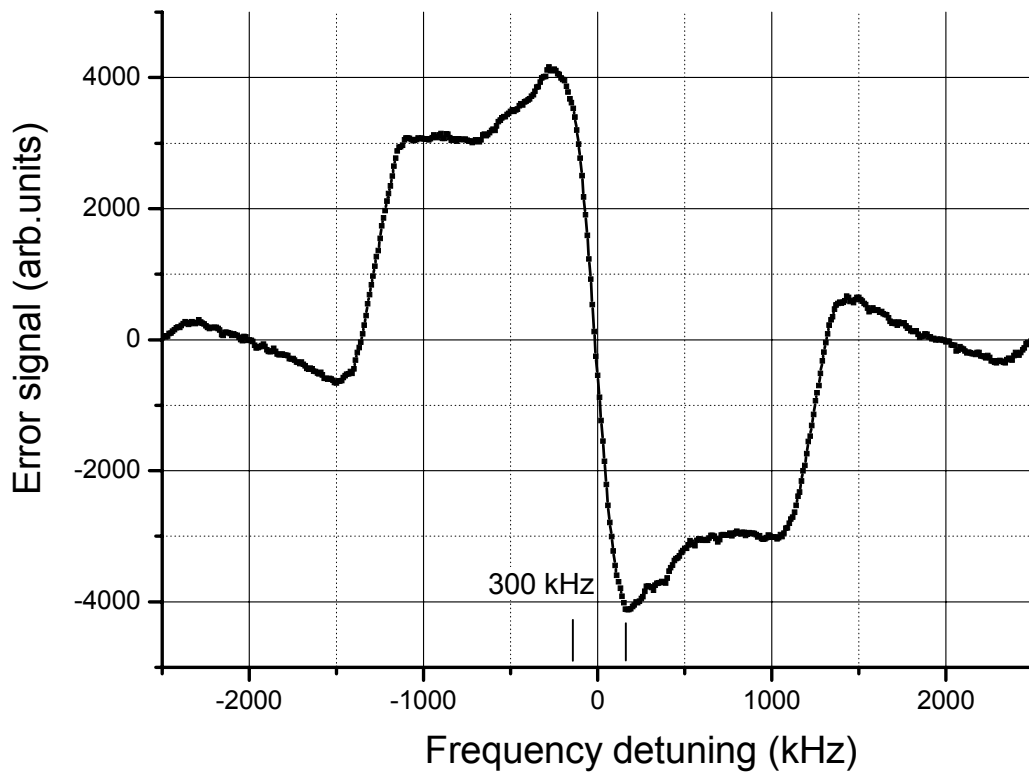


Figure 3

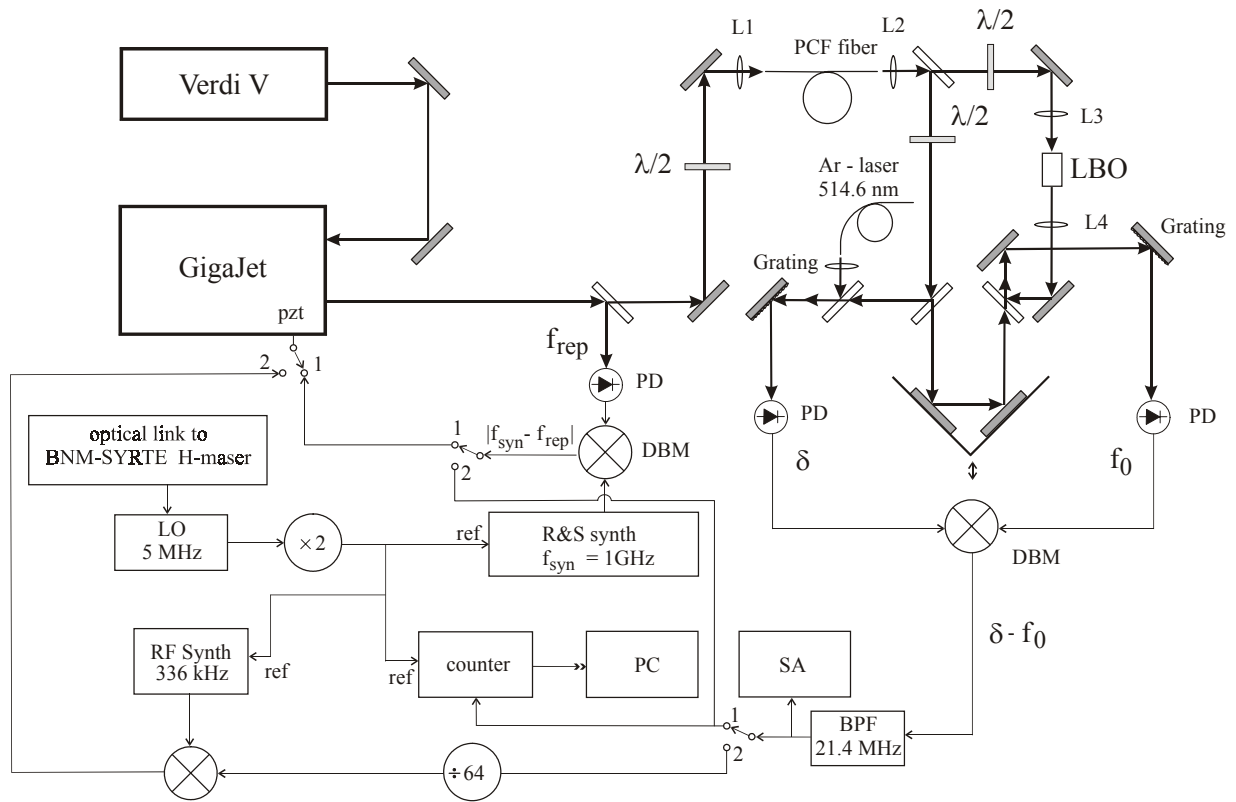


Figure 4

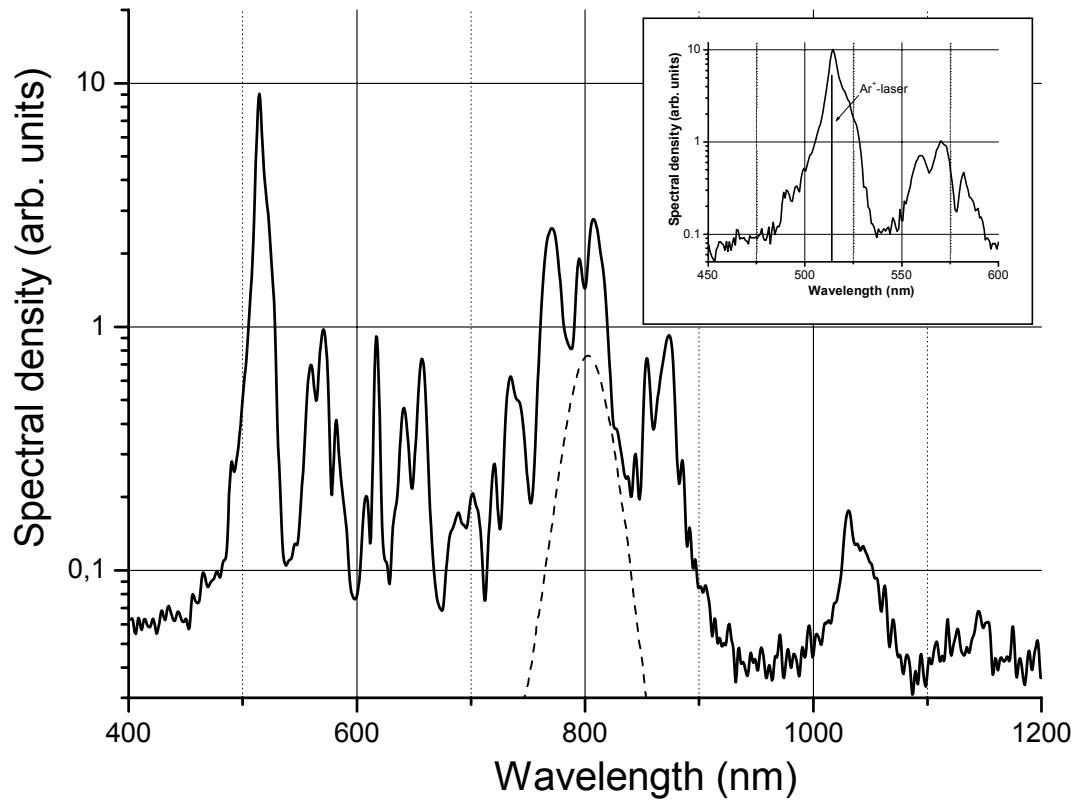


Figure 5

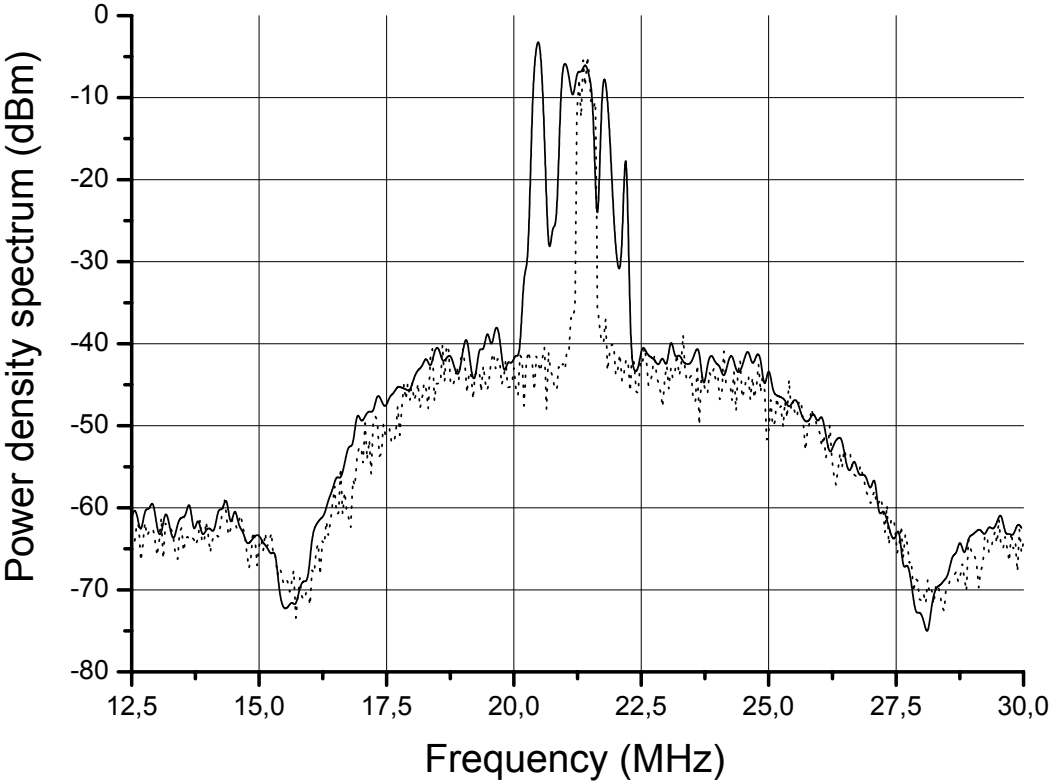


Figure 6

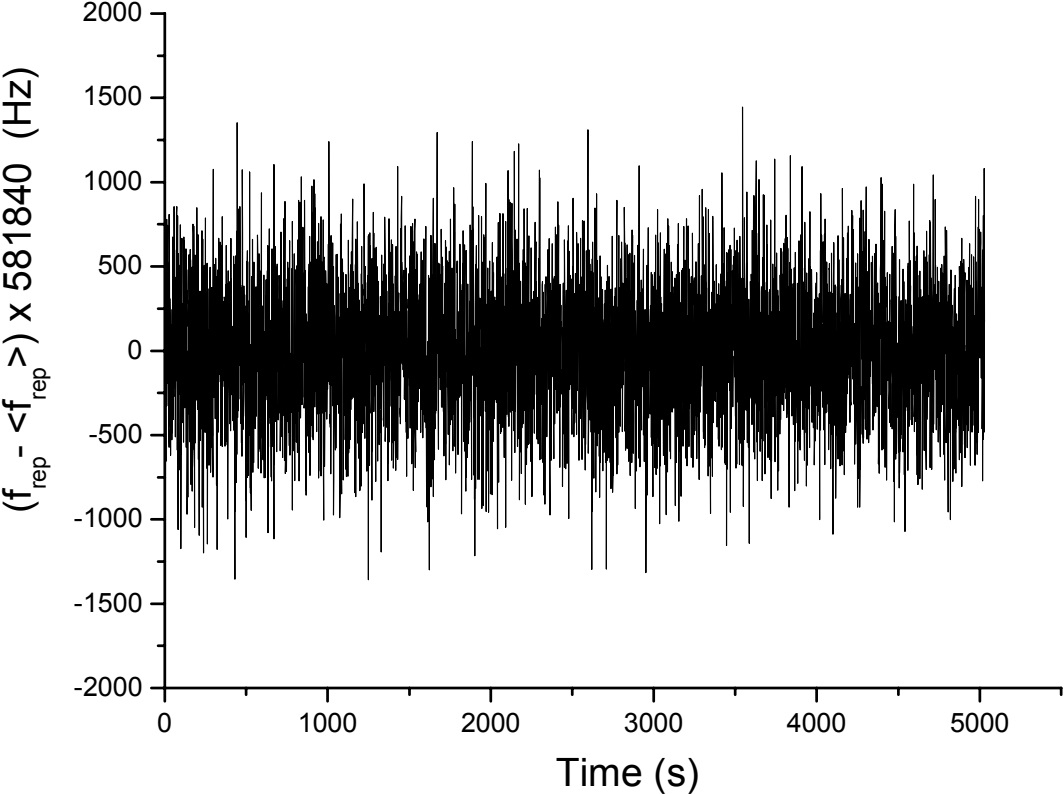


Figure 7

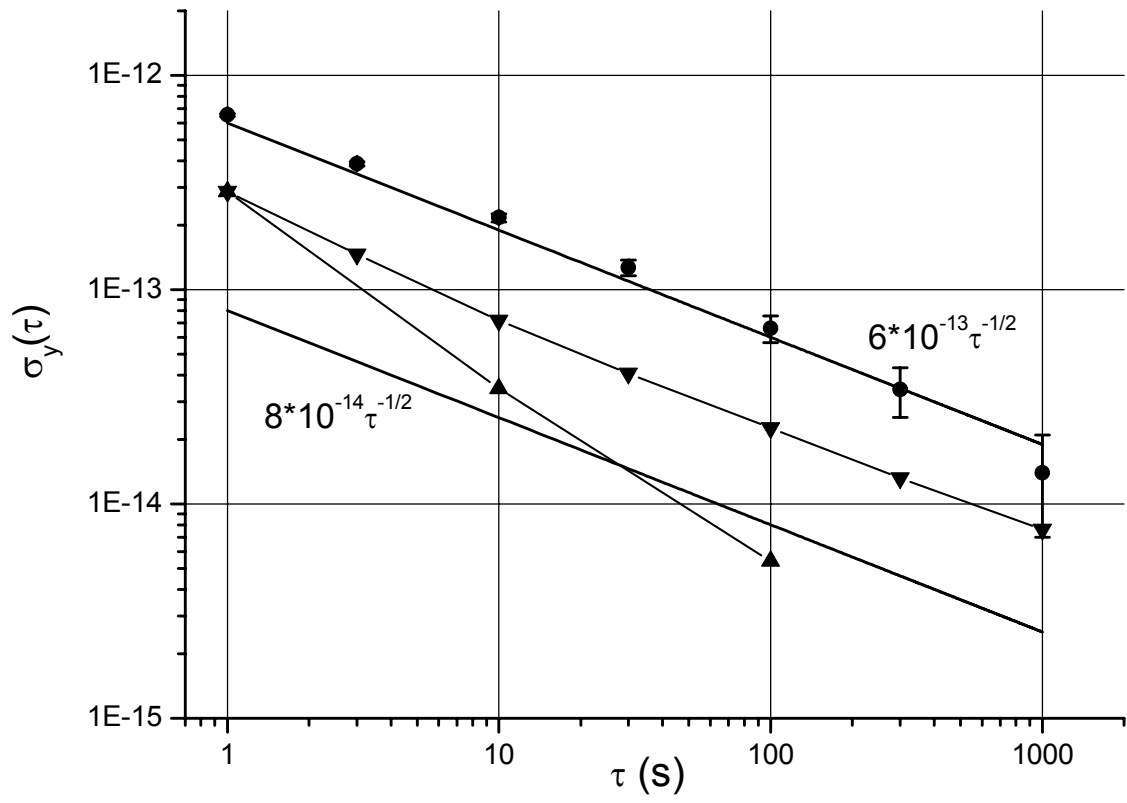


Figure 8

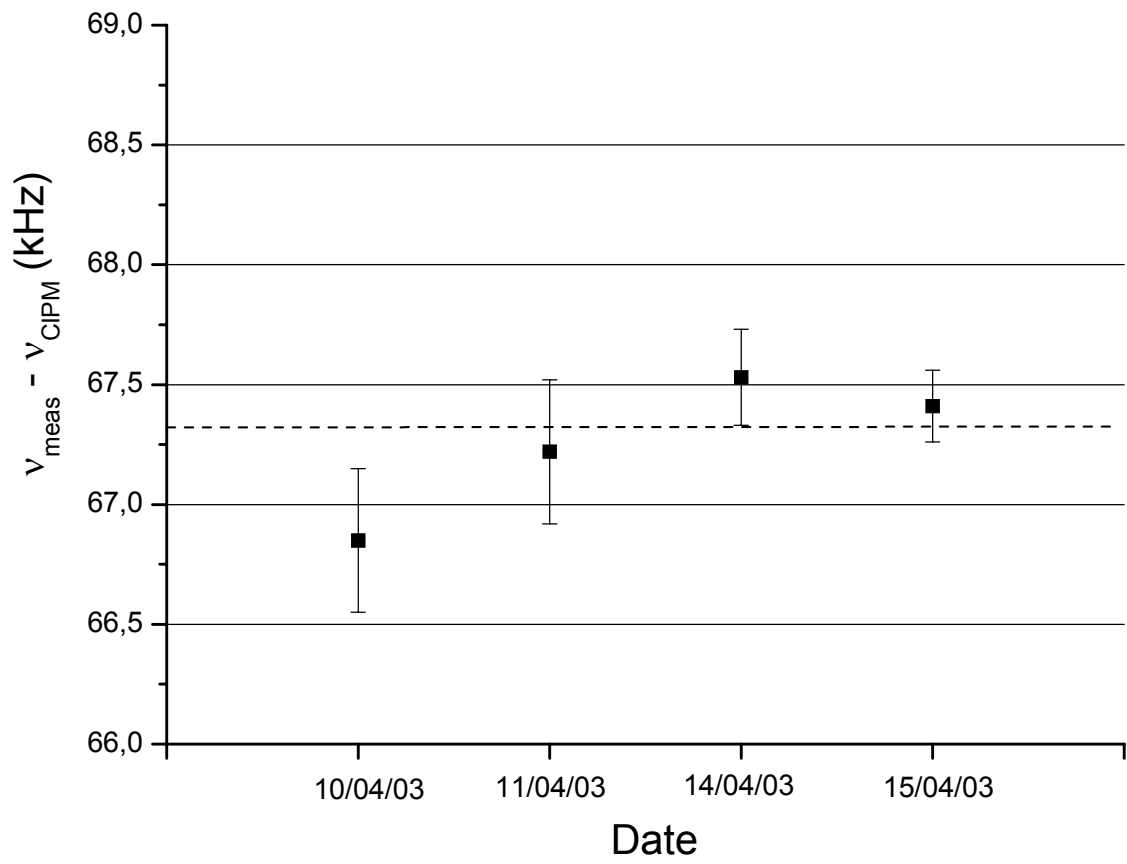


Figure 9

